

# DYNAMICAL FRICTION ON STAR CLUSTERS NEAR THE GALACTIC CENTER

SUNGSOO S. KIM<sup>1</sup>

Kyung Hee University, Dept. of Astronomy & Space Science, Yongin-shi, Kyungki-do 449-701, Korea; sungsoo.kim@khu.ac.kr

AND

MARK MORRIS

Department of Physics & Astronomy, University of California, Los Angeles, CA 90095-1562; morris@astro.ucla.edu

## ABSTRACT

Numerical simulations of the dynamical friction suffered by a star cluster near the Galactic center have been performed with a parallelized tree code. Gerhard (2001) has suggested that dynamical friction, which causes a cluster to lose orbital energy and spiral in towards the galactic center, may explain the presence of a cluster of very young stars in the central parsec, where star formation might be prohibitively difficult owing to strong tidal forces. The clusters modeled in our simulations have an initial total mass of  $10^5$ – $10^6 M_\odot$  and initial galactocentric radii of 2.5–30 pc. We have identified a few simulations in which dynamical friction indeed brings a cluster to the central parsec, although this is only possible if the cluster is either very massive ( $\sim 10^6 M_\odot$ ), or is formed near the central parsec ( $\lesssim 5$  pc). In both cases, the cluster should have an initially very dense core ( $> 10^6 M_\odot \text{pc}^{-3}$ ). The initial core collapse and segregation of massive stars into the cluster core, which typically happens on a much shorter time scale than that characterizing the dynamical inspiral of the cluster toward the Galactic center, can provide the requisite high density. Furthermore, because it is the cluster core which is most likely to survive the cluster disintegration during its journey inwards, this can help account for the observed distribution of presumably massive He I stars in the central parsec.

*Subject headings:* stellar dynamics — Galaxy: center — Galaxy: kinematics and dynamics — galaxies: star clusters — methods: N-body simulations

## 1. INTRODUCTION

The luminosity of the central parsec of our Galaxy is dominated by a cluster of very young stars, including more than a dozen very luminous He I emission-line stars (Krabbe et al. 1995; Paumard et al. 2001) and many O and B stars (Eckart, Ott, & Genzel 1999). Krabbe et al. (1995) find that the properties of the massive, early-type stars in the central parsec can be accounted for by a burst of star formation between 3 and 7 Myr ago. The He I stars appear to be very massive ( $> 40 M_\odot$ ) stars at the luminous blue variable phase or Wolf-Rayet stage, consistent with stellar ages of  $\sim 5$  Myr (Paumard et al. 2001). A total of 16 He I stars are now known within the central parsec, and there are very few He I stars outside this region, other than in two very young star clusters at least 30 pc from the Galactic center (described below). Only one emission-line star has been reported between radii of 1 and 5 parsecs (Cotera et al. 1999).

Such extremely young ages suggest *in situ* formation for the cluster. However, the very strong tidal forces there raise the question of whether the gas density can reach the limiting Roche value. While the maximum gas density in the central parsec, a few times  $10^6 \text{cm}^{-3}$  (Jackson et al. 1993), currently appears to be substantially lower than the minimum density required for a cloud to remain bound,  $\sim 6 \times 10^7 \text{cm}^{-3}$  (Morris 1993), little can now be said about the conditions there when the central cluster formed. One possibility is that the gravitational collapse leading to the formation of the present cluster of young stars in the central parsec was triggered by in-fall of a particularly dense gas cloud, which experienced

compression by shocks involving cloud-cloud collisions, self-intersecting gas streams, or violent explosions near or at the central black hole (Morris 1993; Sanders 1998; Morris, Ghez & Becklin 1999). The possibility that the He I stars in the central parsec are something more exotic than massive, windy stars, such as Thorne-Zytkow type objects, was also considered by Morris (1993), who invoked the large stellar number density there to argue that mergers between compact stellar remnants and normal stars might have given rise to such a population. However, the subsequent finding that He I stars are found in other massive stellar clusters in the Galactic center region (e.g., the Quintuplet Cluster; Figer, McLean, & Morris 1999) eliminated the rationale for that hypothesis.

Alternatively, the star cluster could have formed outside the central parsec, where tidal forces are relatively weaker and star formation is consequently less problematic, and later migrated into the Galactic center (GC) (Gerhard 2001). This idea is motivated by the presence of two other massive, young star clusters near the GC, the “Arches cluster” (Nagata et al. 1995; Cotera et al. 1996; Figer et al. 1999) and the “Quintuplet cluster” (Okuda et al. 1990; Nagata et al. 1990; Glass, Moneti, & Moorwood 1990; Figer et al. 1999), both lying within  $\sim 35$  pc, in projection, of the GC. These clusters are only 2–5 Myr old and contain very luminous emission-line stars similar to those in the central parsec (Figer, McLean, & Morris 1995; Figer et al. 1999). Gerhard (2001) proposes that dynamical friction can bring a massive young star cluster, initially embedded in its parent molecular cloud, into the central parsec during the lifetime of its most massive stars, depending on the initial

<sup>1</sup> Also at Institute of Natural Sciences, Kyung Hee University

location and mass of the cluster. The drag force represented by dynamical friction, acting in the direction opposite to the cluster motion, is owed to the induced “wake” of background stars. If the star cluster is massive enough, the resulting deceleration can in principle be large enough to cause the cluster to spiral into the GC.

When the original Chandrasekhar formula for deceleration by dynamical friction (Chandrasekhar 1943) is applied to the Arches and Quintuplet clusters, both of which are estimated to have had an initial cluster mass of several  $10^4 M_\odot$  (Figer et al. 1999; Kim et al. 2000), one arrives at a timescale of  $\sim 100$  Myr for them to spiral into the GC. Even with initial cluster mass of  $10^5 M_\odot$ , the friction timescale  $\tau_{fric}$  would not be shorter than 30 Myr, which is much longer than the lifetimes of the He I stars within the central parsec. Gerhard (2001), however, finds much smaller time scales for the cluster migration by assuming much larger cluster masses, or by considering that the parent molecular cloud might stay bound to the cluster so that the effective cluster mass is large enough to yield a suitably short dynamical friction time scale. He finds that a massive cluster and its associated cloud, with combined mass of  $10^6 m_6 M_\odot$  and galactocentric radius of  $\leq 30 m_6^{1/2}$  pc will reach the central parsec within the lifetime of the He I stars observed in the central parsec.

Numerical simulations of dynamical friction for globular clusters or satellite galaxies in the galactic halo have shown that the Chandrasekhar formula provides an accurate description for the orbital motion of a body experiencing dynamical friction (e.g., White 1976; Lin & Tremaine 1983). However, the formula describes the orbiting cluster as a single, rigid particle, while an actual star cluster has a rather smooth, extended density profile and gradually loses its stars beyond the tidal radius. Near the GC, the tidal radius is small (compared to the cluster mass) enough to be an important determinant of the cluster fate (Kim et al. 1999, 2000). Using a simple assumption for the density profile of the cluster (an isothermal sphere with a tidal cutoff), Gerhard modified the Chandrasekhar formula to take this effect into account. However, the behavior of stars near and outside the tidal radius of the cluster is rather difficult to describe, and the “lingering time” of those stars is found to often be much longer than the dynamical timescale of the cluster (Fukushige & Heggie 2000; Takahashi & Portegies Zwart 1998).

Furthermore, the tidal radius of the cluster continuously shrinks as the cluster approaches the GC, and the cluster will eventually disrupt. The distribution of cluster members in galactocentric radius after the disruption will be determined by the galactocentric radius at which the cluster disrupts, by the deviation of the cluster’s orbital motion from circularity, and by the shape of the gravitational potential of the Galaxy. The final distribution of the remnant stars is an important issue because most clusters will begin to disrupt before reaching the central parsec, and even for those which do survive as a separate entity and reach the central parsec, the kinetic energies of the remnant stars after disruption may be large enough that they are not bound inside the central parsec. Therefore, the final fate of a cluster experiencing

TABLE 1. GALAXY MODELS

Model	$R_{trunc}$ (pc)	$R_{out}$ (pc)	$M_{galaxy}^a$ ( $M_\odot$ )	$N_{galaxy}^b$
1	80	120	$3.1 \times 10^8$	$2 \times 10^6$
2	15	25	$4.3 \times 10^6$	$2.8 \times 10^5$
3	20	30	$6.0 \times 10^6$	$4 \times 10^5$

<sup>a</sup>Total mass of the galaxy particles

<sup>b</sup>Total number of galaxy particles

dynamical friction can only be learned using numerical simulations, which can take these myriad and complex effects into account.

We have carried out numerical simulations of the orbital and structural evolution of star clusters situated in a realistic Galactic potential in order to further explore the hypothesis that star clusters can be brought into the center by dynamical friction, to accurately determine the timescales characterizing the process, and to predict the final distribution of remnant stars after disruption. We judge it likely that the parent molecular cloud will be separated from the star cluster relatively shortly after cluster formation<sup>2</sup>, so we do not consider the parent cloud in our simulations. We confirm that it is possible for the ‘central parsec cluster’ to have resulted from a star cluster formed outside the central parsec and brought inwards by dynamical friction. However, the constraints imposed by this mechanism appear to be rather severe: the cluster must either begin its journey quite close to the GC, or be much more massive than any currently observed cluster, or both.

Our models and the method of simulation are described in § 2, and the simulation results are presented and discussed in § 3. Our findings are then summarized and discussed in § 4.

## 2. MODELS

### 2.1. The Code

For the simulations presented here, we use an N-body/SPH (Smoothed Particle Hydrodynamics) code named GADGET, which is freely available at <http://www.mpa-garching.mpg.de/gadget> (Springel, Yoshida, & White 2001). GADGET computes gravitational forces with a hierarchical tree algorithm and represents fluids by means of SPH. The code uses individual and adaptive timesteps for all particles. We adopted a parallelized version of GADGET, which implements the standardized MPI (Message Passing Interface) communication interface, and we use only the gravitational part of the code. The code is thus effectively a gravitational N-body code, with no hydrodynamical effects included.

### 2.2. The Galaxy

<sup>2</sup> Some mechanisms for the loss of angular momentum apply only to the gas component, such as cloud collisions and other viscous interactions with the interstellar medium, as well as magnetic viscosity (Morris & Serabyn 1996). Also, the radiation pressure from a massive cluster can exert sufficient force to separate cluster and cloud on a relatively short time scale, if the cluster is not located exactly at the center of the cloud.

We adopt a truncated, softened, spherical, power-law density profile for the central region of the Galaxy:

$$\rho_g = \frac{4 \times 10^6}{1 + (R/0.17 \text{ pc})^{1.8}} \exp(-(R/R_{trunc})^6) \text{ M}_\odot \text{pc}^{-3}. \quad (1)$$

This is a density model from Genzel et al. (1996) with an added exponential truncation. By introducing such truncation, rather than using a simple cutoff at the outer boundary, we were able to significantly reduce numerical inaccuracies involved in converting the density profile to the distribution function (see below). Depending on the initial  $R$  (galactocentric radius) of the cluster, we use values 15–80 pc for the truncation radius,  $R_{trunc}$ , which are set to be 2.5 to 6 times larger than the initial  $R$  in order to ensure suitable representation of the Galaxy particles outside the initial  $R$  of the cluster. The outer boundary of the Galaxy,  $R_{out}$ , is set to be 50 % larger than  $R_{trunc}$ . Table 1 shows three sets of  $R_{trunc}$  and  $R_{out}$  used in our simulations.

For the non-rotating Galaxy model, the system is assumed to be in equilibrium, and to have an isotropic velocity distribution. We thus obtain the distribution function by integrating the Eddington formula (Binney & Tremaine 1987). The initial positions and velocities of the particles representing the Galaxy are then determined from the distribution function in a Monte Carlo fashion.

Some of our simulations implement a rotating Galaxy model. In order to produce an equilibrated rotating Galaxy model, we simply “flip” the sign (take the absolute value) of the azimuthal velocity component (that about the rotation axis) for a certain fraction of particles whose locations and original velocities were chosen as just described. This technique, developed by Lynden-Bell (1960), produces a rotating system without requiring modification of either its total potential and kinetic energies or the ratio between its radial and tangential velocities. Lindqvist, Habing, & Winnberg (1992) showed that the average radial velocity  $\bar{v}_r$  of OH/IR stars in the central  $\sim 100$  pc of the Galaxy can be fit by a relation  $\bar{v}_r = 1.1 \text{ km/s}(l/\text{pc}) + c$  with an average dispersion of 82 km/s, where  $l$  is the Galactic longitude and  $c$  is a constant close to 0. We find that the observed rotational characteristics of the OH/IR stars can be well reproduced by flipping the following fraction of particles,  $f_{flip}$ , expressed as a function of galactocentric radius projected onto the plane normal to the rotation axis,  $R_p$ :

$$f_{flip} = \min [0.4(R_p/30 \text{ pc}), 1]. \quad (2)$$

We use this fraction for our rotating Galaxy models.

Depending on  $R_{trunc}$ , we use  $2.8 \times 10^5$ ,  $4 \times 10^5$ , or  $2 \times 10^6$  particles to model the Galaxy, but the mass represented by a single particle is always  $\sim 150 \text{ M}_\odot$ . To model the compact, massive object at the center of the Galaxy, one particle with mass  $2.5 \times 10^6 \text{ M}_\odot$  is put at the center of the system.

The Galaxy in our simulations can be regarded as a collisionless system for the time intervals considered here. A particle-based method like GADGET requires softening of gravity to better describe collisionless systems. However, determining the most appropriate softening length,  $\epsilon$ , for a given problem and method is not trivial. If  $\epsilon$  is too small, unphysical relaxation would take place, and if

too large, a given galactic density distribution would not be properly represented. There seems to be no universal way to find the “optimal softening”, and each problem/method requires a series of experiments to obtain its own optimal value (Merritt 1996; Athanassoula et al. 2000; among others). Our experiments without a cluster component indicate that 0.3 pc for Galaxy model 1 and 0.1 pc for Galaxy models 2 & 3 are the minimum  $\epsilon$  values that result in an acceptably small temporal deviation in density profile for the region of interest and the time interval covered. Because the majority of particles that induce dynamical friction on a cluster are outside the tidal radius of the cluster, and because adopted values of  $\epsilon$  in our models are always smaller than the tidal radii of the clusters, the choice of  $\epsilon$  will not significantly affect the dynamical friction time scales that result from our models.

The experiments showed that for Galaxy model 1, the density profile remained nearly constant over time for  $R > 2$  pc, and for Galaxy models 2 & 3, the enclosed mass did not vary by more than 10 % everywhere, for the time interval covered in our simulations. A slight density enhancement inside 1 pc ( $\sim 20$  % at 1 pc) was observed during the simulation for Galaxy models 2 & 3, which seems to be due to the numerical inaccuracies introduced by the large mass ratio between the Galaxy particles and the black hole particle. However, in that central region, the uncertainty is dominated by the estimation of the density profile in that region, so the density enhancement should not affect the scientific results given in the present paper. We set the  $\epsilon$  value of the black hole particle to be the same as the Galaxy particles.

### 2.3. The Cluster

We initially model the cluster with the Plummer density profile,

$$\rho_{cl} = \frac{M_{cl}}{4\pi r_c^3} \left(1 + \frac{r^2}{r_c^2}\right)^{-5/2}, \quad (3)$$

where  $M_{cl}$  is the cluster mass and  $r_c$  the cluster core radius. The locations and velocities of cluster particles are chosen using this profile in the same manner as for the Galaxy particles.

Clusters in our simulations have a total mass of either  $10^5 \text{ M}_\odot$  or  $10^6 \text{ M}_\odot$ . We set a cluster particle to represent  $10 \text{ M}_\odot$ , so the number of particles for a cluster is  $10^4$  or  $10^5$ .

GADGET is not designed to handle details of the internal dynamics of star clusters such as close encounters between stars/binaries, and thus it cannot accurately describe the dynamical evolution of star clusters. The dynamical evolution may be important for our lower mass ( $10^5 \text{ M}_\odot$ ) clusters, and we will discuss this more §4) We find that  $\epsilon$  of 0.025 pc is an appropriate softening length for the cluster particles. This value keeps our clusters approximately stationary for the time intervals investigated. This softening value is applied only between cluster particles. For interactions between particles representing different components, GADGET uses the larger of the two softening lengths (for our models,  $\epsilon$  for the galaxy particles is always larger than that for the cluster particles).

Although we use a fairly large number of particles for the Galaxy, Poisson noise could be problematic at large

TABLE 2. SIMULATION PARAMETERS

Simulation	$R$ (pc)	$v_{init}^a$ ( $v_{circ}^b$ )	$M_{cl}$ ( $M_\odot$ )	$N_{cl}$	$r_c$ (pc)	$r_t/r_c$	$\rho_c$ ( $M_\odot \text{pc}^{-3}$ )	Galaxy Rotation	Galaxy Model
1	30	1	$10^6$	$10^5$	0.86	6	$1.3 \times 10^5$	N	1
2	30	0.5	$10^6$	$10^5$	0.86	6	$1.3 \times 10^5$	N	1
3	30	0.5	$10^6$	$10^5$	0.86	6	$1.3 \times 10^5$	Y	1
4	30	0.5	$10^6$	$10^5$	0.28	19	$3.8 \times 10^6$	N	1
5	5	0.5	$10^6$	$10^5$	0.28	6	$3.8 \times 10^6$	N	2
6	10	0.5	$10^6$	$10^5$	0.43	6	$1.0 \times 10^6$	N	3
7	10	0.5	$10^6$	$10^5$	0.28	9.3	$3.8 \times 10^6$	N	3
8	5	0.5	$10^5$	$10^4$	0.13	6	$3.8 \times 10^6$	N	2
9	2.5	0.5	$10^5$	$10^4$	0.080	6	$1.6 \times 10^7$	N	2
10	2.5	0.5	$10^5$	$10^4$	0.039	12	$1.3 \times 10^8$	N	2
11	2.5	1	$10^5$	$10^4$	0.039	12	$1.3 \times 10^8$	N	2
12	5	0.5	$10^5$	$10^4$	0.039	20	$1.3 \times 10^8$	N	2
13	10	0.5	$10^5$	$10^4$	0.039	30	$1.3 \times 10^8$	N	3

<sup>a</sup>Initial cluster velocity<sup>b</sup>Circular velocity at a given  $R$ 

$R$  or in regions of low  $\rho_g$  (the average distance between particles of Galaxy model 1 at  $R = 30$  pc is  $\sim 0.9$  pc). For example, since we model the cluster as a system of particles, rather than as a point source, Poisson noise in the Galaxy potential could conceivably heat the cluster and affect its internal structure. However, we find that during its first revolution period, our cluster with  $M_{cl} = 10^6 M_\odot$ , in a circular orbit located at  $R = 30$  pc (the largest  $R$  among our simulations), maintained a roughly steady density profile and mean velocity dispersion (within a few percent). We thus believe that the effect of Poisson noise from our Galaxy model on the cluster is negligible.

### 3. RESULTS

#### 3.1. $10^6 M_\odot$ Clusters

In order to search for the parameters that may bring a cluster to the GC within several Myr via dynamical friction, we start our simulations with a significantly more massive version of the Arches & Quintuplet clusters. Simulation 1 has a cluster having a total initial mass of  $M_{cl} = 10^6 M_\odot$ , a Plummer core radius of  $r_c = 0.86$  pc, and a circular orbit at  $R = 30$  pc. Although we adopted a Plummer model for clusters for the sake of simplicity, equilibrium clusters located in an external tidal field are better represented by King models (King 1966). The Plummer model does not have an intrinsic tidal limit, but the tidal radius,  $r_t$ , can be defined by

$$r_t \equiv \left( \frac{M_{cl}}{2M_g} \right)^{1/3} R, \quad (4)$$

where  $M_g$  is the Galaxy mass enclosed inside  $R$ . The Plummer model with a ratio  $r_t/r_c$  of 6 has core density and half-mass radius comparable to those of the King model with  $W_0 = 4$  (isotropic King models have only one parameter,  $W_0$ , the concentration parameter;  $W_0 = 4$  represents a moderate concentration). The tidal radius at  $R = 30$  pc for a  $M_{cl} = 10^6 M_\odot$  cluster is 5.1 pc, so  $r_t/r_c = 6$  for Simulation 1, which represents an equilibrated cluster having a moderate concentration and filling its tidal radius.

Figure 1 shows the evolution of Simulation 1. It takes  $\sim 12$  Myr for the cluster to reach  $R = 9$  pc, where

the cluster completely disrupts, i.e., the core density ( $\rho_c$ ) becomes smaller than the local background density,  $\sim 3 \times 10^3 M_\odot \text{pc}^{-3}$ .

The mechanism that triggers cluster formation, such as a cloud-cloud collision, could dissipate some of the original energy of bulk motion into a less ordered form such as turbulence or thermal energy. This would lead to an eccentric initial orbit for the cluster. Since an eccentric orbit would expose a cluster to a higher background stellar density at an earlier phase, the cluster will experience relatively stronger dynamical friction effects during a given time interval. Here we test this notion by trying in Simulation 2 a rather extreme example of an eccentric orbit: we set the cluster to initially have a purely tangential velocity equal to half of the circular velocity ( $v_{circ}$ ) at the initial  $R$ . All our eccentric orbits in the present paper will have these conditions. Simulation 2 otherwise has the same parameters as Simulation 1.

This orbit of Simulation 2 plunges the cluster from  $R = 30$  pc to 10 pc in 0.4 Myr. Figure 1 shows the orbital motion of the cluster center. As a result of the eccentric initial orbit, the time to total disruption has significantly decreased: we find that the density of the cluster core becomes smaller than the background density at  $\sim 5$  Myr. It is notable that, in both Simulations 1 & 2, the cluster core disrupts when it reaches  $R \simeq 10$  pc.

The center of the now unbound cluster continues to oscillate in  $R$  even after total disruption for a while ( $t > 5$  Myr), but the minimum  $R$  does not vary significantly afterwards. In fact, for this later period, our definition of the density center of the cluster is simply the average position of a group of particles that were bound to the cluster just prior to disruption, and thus the center becomes meaningless after the stars later become phase-mixed in their orbits. At these later stages, the full distribution of the cluster particles is more important for understanding the fate of the cluster. Figure 2a displays the evolution of the radial distribution of cluster particles (left panel), and a histogram of the radial distribution at the final simulation step (right panel). After the disruption, the histogram peaks near  $R = 10$  pc and has a rather distinct inner boundary at  $R = 3$  pc. These

results show that the eccentric initial orbit can shorten  $\tau_{fric}$  but it does not help in allowing the cluster to penetrate deeper into the GC before disruption.

The Chandrasekhar formula states that the drag force is inversely proportional to the second power of the dispersion of the relative velocity between the cluster and the background stars. Thus, if the background stellar system has a net rotation and the cluster rotates in the same manner, then the relative velocity will be smaller and the effects of dynamical friction will be larger. Indeed, the central region of the Galaxy does rotate (see § 2.2), although fairly weakly. Simulation 3 is an attempt to assess the effect of such rotation on dynamical friction. Figure 1 shows that cooperative Galactic rotation only slightly enhances the friction effect, i.e., it brings the cluster inward more quickly by just a fraction of a Myr. We find that the final stellar distributions of Simulations 2 and 3 are very much alike.

The three simulations discussed above disrupt at nearly the same  $R$ . Aside from  $M_{cl}$  and  $R$ , the core radius  $r_c$  is the only common initial parameter among the three simulations. To investigate the dependence of the final  $R$  on the initial  $r_c$ , we perform Simulation 4, which initially has  $r_c = 0.28$  pc, about 1/3 of that in Simulations 1–3. This gives  $r_t/r_c = 19$ , and a central density of  $3.8 \times 10^6 M_\odot \text{pc}^{-3}$  (30 times that of the previous simulations). This density is 1 to 2 orders of magnitude larger than the typical central density of Galactic globular clusters.

The temporal progression of the density distribution in galactocentric radius for this simulation is shown in Figure 2b. Despite its relatively large initial core density, the cluster again disrupts before reaching the central parsec. However, the final stellar distribution does peak at smaller  $R$  ( $\sim 5$  pc) than Simulations 1–3 ( $\sim 10$  pc). This is because clusters having a larger central density can survive in the presence of larger background densities.

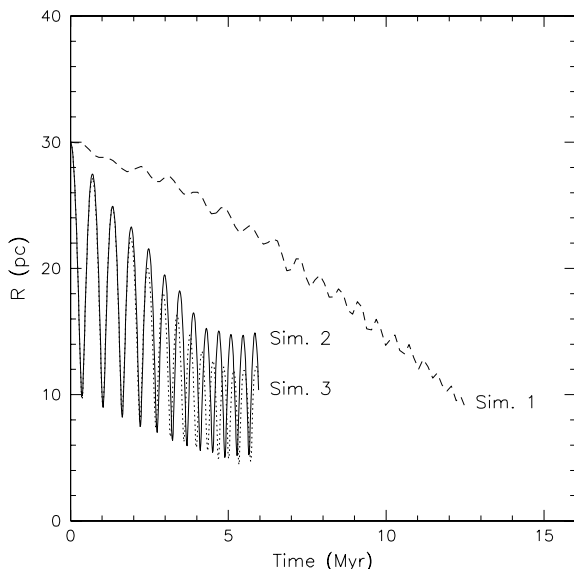


FIG. 1.— Radial ( $R$ ) evolution of the center of the cluster for Simulations 1 (dashed line), 2 (solid line), and 3 (dotted line).

Nonetheless, it is clear that the simulations discussed so far do not deliver massive stars into the central parsec.

Now we move the initial  $R$  closer to the GC. Simulation 5 assumes the same cluster as Simulation 4, but placed initially in an eccentric orbit at  $R = 5$  pc. As shown in Figure 2c, the cluster of Simulation 5 finally reaches the central parsec and the core disrupts there. However, after the complete disruption, more than 60 % of the cluster members are located outside the central parsec at any given time. On the other hand, the histogram for the stars that initially constituted the central 1 % of the cluster shows that 70 % of those stars end up projected inside the central parsec at the final stage (thin line in the right panel). This fraction increases to 90 % when projected onto the sky. Thus, if the progenitors of the He I stars are initially located at the core of the cluster, simple binomial statistics give a probability of  $\sim 19$  % for the 16 known He I stars to be found within the central parsec at any given moment after disruption. This probability is large enough that we identify Simulation 5 as a candidate for the central parsec cluster.

The idea of an initial mass segregation of heavier stars is consistent with some cluster formation models such as the one by Murray & Lin (1996), where encounters between cloudlets increase the protostellar masses, and the one by Bonnell et al. (1997), in which the deeper potential in the core causes stars there to accrete relatively greater amounts of circumstellar material. In addition, due to their compactness (large overall densities), clusters formed near the Galactic center may undergo extremely rapid mass segregation in the beginning of the evolution (Kim et al. 1999; this segregation is not observed in our simulations because our cluster particles have the same mass and more importantly, the internal dynamical evolution of the cluster has been suppressed by giving non-negligible  $\epsilon$  values to the cluster particles.). Thus, the initial mass segregation due to internal dynamics will preferentially bring massive stars to the central parsec.

To see if a cluster can reach the central parsec from a greater distance, we initially locate the clusters of Simulations 6 and 7 at  $R = 10$  pc. Simulation 6 has the standard initial concentration,  $r_t/r_c = 6$ , while Simulation 7 has a higher concentration,  $r_t/r_c = 9.3$  (notice that Simulation 7 has the same  $\rho_c$  as Simulation 5). Figures 2d & e show that Simulation 6 results in a stellar disruption that leaves stars widely distributed from 0.5 to 4 pc, and that the final phase of Simulation 7 resembles that of Simulation 5. 90 % of the central 1 % of stars initially in the core of Simulation 7 are found within the central parsec of the projected sky at the final stage. As can be seen in the comparison between Simulations 5 and 7, it appears that the final distribution of stars is mainly determined by the initial  $\rho_c$  (or, in more realistic clusters in which relaxation processes are possible, by the  $\rho_c$  that is quickly established by mass segregation). We identify Simulation 7 as another candidate for the central parsec cluster.

There is a potential problem with  $10^6 M_\odot$  cluster models. While their large mass causes the cluster to migrate inwards rapidly, it is then very difficult to match the observed number of He I stars at the GC,  $\sim 16$  (Paumard et al. 2001). Assuming that the progenitors of He I stars have an initial mass  $> 40 M_\odot$ , the Salpeter initial mass

function (IMF) with lower and upper mass boundaries of  $0.1$  and  $150 M_{\odot}$ , respectively, will result in  $\sim 700$  He I stars out of a total mass of  $10^6 M_{\odot}$ . To match the observed number, the power law slope of the IMF needs to be as large as 3 (compared to 2.35 for the Salpeter IMF) all the way down to  $0.1 M_{\odot}$ . A slope of 3 represents an extremely steep IMF, considering that even the disk IMF, which is thought to be significantly steeper than the GC IMF (Morris 1993; Figer et al. 1999; Kim et al. 2000), has a much flatter IMF for  $< 1 M_{\odot}$  (power law slope of 2.1–2.3; Kroupa 2001 and references therein). The assumed lower mass cutoff at  $40 M_{\odot}$  for He I stars is based on the suggestion by Paumard et al. that the GC He I stars are in the luminous blue variable phase or at the Wolf-Rayet stage. If the lower mass cutoff for the helium emission-line stars is, for example,  $70 M_{\odot}$ , the number of He I stars would be  $\sim 250$ . On the other hand, if some of more massive He I stars, for example, those initially having  $> 60 M_{\odot}$ , have already undergone supernova explosions, the number of remaining He I stars would be  $\sim 350$  (the calculations by Schaller et al. 1992 give 3.9 and 4.8 Myr for the lifetimes of solar-metallicity [ $z = 0.02$ ] stars with initial masses of  $40 M_{\odot}$  and  $60 M_{\odot}$ , respectively). However, these numbers are still significantly larger than the observed number.<sup>3</sup>

We have therefore investigated one more group of clusters: clusters with a smaller initial  $M_{cl}$  ( $10^5 M_{\odot}$ ) starting at closer  $R$  ( $\leq 10$  pc).

### 3.2. $10^5 M_{\odot}$ Clusters

For a Salpeter IMF and mass limits of  $0.1$ – $150 M_{\odot}$ , a cluster having  $M_{cl} = 10^5 M_{\odot}$  will yield  $\sim 35$  stars with masses between  $40 M_{\odot}$  and  $60 M_{\odot}$ , which is now much closer to the number of He I stars observed in the central parsec.

Simulations 8 and 9 have a moderate initial concentration of  $r_t/r_c = 6$  (but relatively high  $\rho_c$  of  $3.8 \times 10^6$  and  $1.6 \times 10^7 M_{\odot} \text{pc}^{-3}$ ), and an eccentric initial orbit starting at  $R = 5$  and  $2.5$  pc, respectively. As shown in Figures 2f & g, it takes only a fraction of a Myr for these clusters to completely disrupt, and the final stellar distributions are not confined to the central parsec. While the peak of the final radial distribution of cluster stars in Simulation 9 is just inside the central parsec, most particles of Simulation 8 are located outside the central parsec. These clusters, although started at fairly small values of  $R$ , will not look like the central parsec cluster, for which even higher initial  $\rho_c$  will be required.

As an extreme case, we set Simulation 10 to have  $r_t/r_c = 12$  and an eccentric initial orbit at  $R = 2.5$  pc. This cluster will initially have  $\rho_c$  of  $1.3 \times 10^8 M_{\odot} \text{pc}^{-3}$ , which is an extremely high value. Although it is highly questionable whether a cluster could form with such a high central density, we note that this assumption can be made in compensation for the fact that our single-stellar-mass cluster models necessarily neglect the probably important process of dynamical mass segregation for the Galactic center clusters (Figer et al. 1999; Kim et al. 2000). Mass segregation would concentrate toward the cluster core exactly those stars which we would iden-

tify with the HeI stars in the central parsec, so its neglect here leads to an underestimate of the degree of concentration of massive stars toward the center after disruption. Our assumption of large initial cluster density, is thus in part aimed at illuminating how mass segregation might affect the hypothesis being investigated in this paper. Figure 2h shows that this cluster disrupts within only 1 Myr, inserting 49 % of its members inside the central parsec. When projected onto the sky, 64 % of the stars are found in the central parsec at the final stage. This fraction is somewhat smaller than those of Simulations 5 and 7, and the probability for 16 or so He I stars to be found within the central parsec at any given epoch after disruption would be only  $\sim 0.1$  %.

Unlike Simulations 5 and 7, considering only the initial central 1 % does not increase the final concentration inside the central parsec for Simulation 10. Simulation 11 in Figure 2i shows that this same cluster can end up resembling the final stage of Simulation 10 even with a circular initial orbit, although it takes somewhat longer for it to undergo disruption. 65 % of the stars are found in the projected central parsec at the final stage of Simulation 11.

Although the probability of finding about 16 He I stars inside the central parsec, and none outside this radius, is small for Simulations 10 and 11, the final distributions from these simulations are quite concentrated at the GC. In fact, our simulations, in which internal cluster dynamics are not considered and all cluster particles have the same mass, may not accurately represent the detailed structure of the cluster core, even for cases in which we have augmented the initial core density to artificially allow for mass segregation. Thus, if the extremely compact cluster core consisting of massive stars were to be better modeled, Simulations 10 & 11 may then be able to bring a much higher fraction of core stars down to the central parsec. We thus identify these two simulations as potential candidates for the central parsec cluster.

Finally, we try this dense cluster model at greater initial  $R$ . Simulations 12 and 13 have the same initial central density as Simulation 10, but have greater initial  $R$ 's, 5 and 10 pc, respectively. Figures 2j & k show that the final distributions of Simulations 12 and 13 are similar to that of Simulation 10, although the fraction of stars inside the central parsec for Simulation 13 is slightly smaller ( $\sim 43$  %). This confirms that it is the initial central density, not  $R$ , that mainly determines the fate of the cluster, when only dynamical friction is accounted for (i.e., when internal dynamics is not considered). Note that it takes 1.5 and 4 Myr, respectively, for dynamical friction to bring the clusters in Simulations 12 and 13 into the central parsec.

Unlike our previous simulations, these time scales for dynamical friction are comparable to the time scales by which clusters evaporate by relaxation and stellar mass loss. In particular, for an IMF slope of 2.35, Kim et al. (1999) find that the cluster in Simulation 13 would evaporate within  $\sim 4$  Myr, if it stayed at its initial  $R$ , 10 pc. It is difficult to estimate how important the relaxation will be when the dynamical friction makes the cluster rapidly lose its mass by moving it into a stronger tidal potential (so that the tidal radius becomes smaller). However, it is certain that the cluster models considered in the present study are more enduring than more realis-

<sup>3</sup> One could make this number even smaller by assuming that the He I stars are not only a function of mass, but also a function of the evolutionary phase, though.

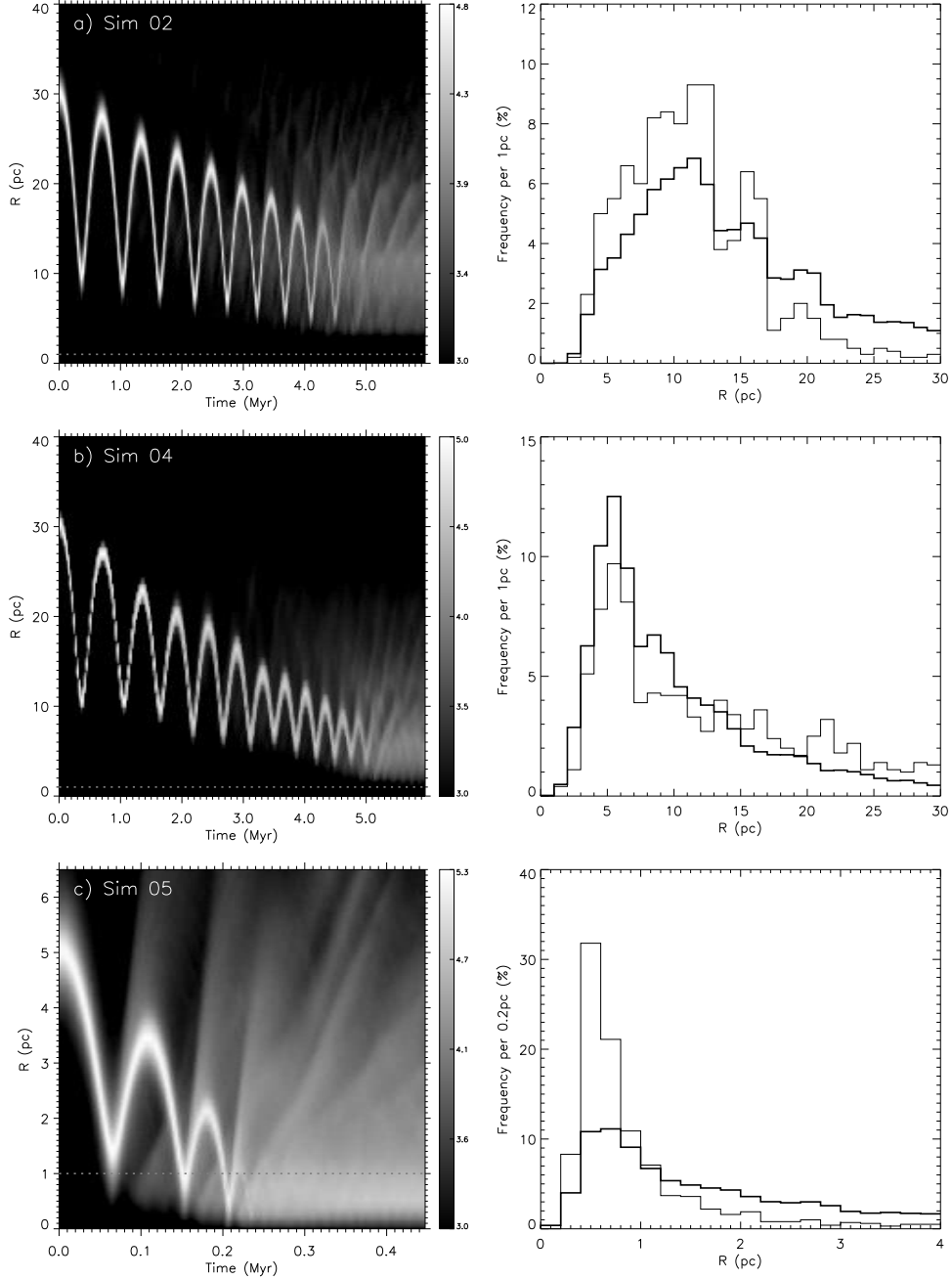


FIG. 2.— Grey scale map for the temporal evolution of number histogram for the radial distribution of cluster particles (*left panels*) and the same histogram for the final simulation step (*right panels*). The grey scale bars next to the maps represent the scales of the density in units of  $M_{\odot}\text{pc}^{-3}$ . In the right panels, thick lines represent all stars in the cluster, and thin lines represent the central 1 % stars at the beginning of the simulation. The horizontal dotted line in the map shows the location of  $R = 1$  pc.

tic models might be, and consequently serve as a useful limiting case.

#### 4. DISCUSSION

We have performed numerical simulations for dynamical friction of star clusters at the Galactic center with  $M_{cl} = 10^5\text{--}10^6 M_{\odot}$  and  $R = 2.5\text{--}30$  pc.

We find that extremely massive versions of the Arches and Quintuplet clusters (Simulations 1–4;  $M_{cl} = 10^6 M_{\odot}$  &  $R = 30$  pc) disrupt before reaching the central parsec. When initially located at  $R \leq 10$  pc, clusters having  $M_{cl} = 10^6 M_{\odot}$  can reach the central parsec within the

estimated age of He I stars,  $\sim 5$  Myr, (Simulations 5 & 7), but the final stellar distribution is spread beyond the central parsec. However, stars initially located at the core of the cluster (as is likely to be the case for He I stars, which are massive enough to sink rapidly to the cluster core soon after formation) tend to be more concentrated in the central parsec at the final stage: of the initially innermost 1% of the cluster stars, 90 % of them end up projected onto the central parsec in Simulations 5 & 7, which we identify as candidates for the central parsec cluster.

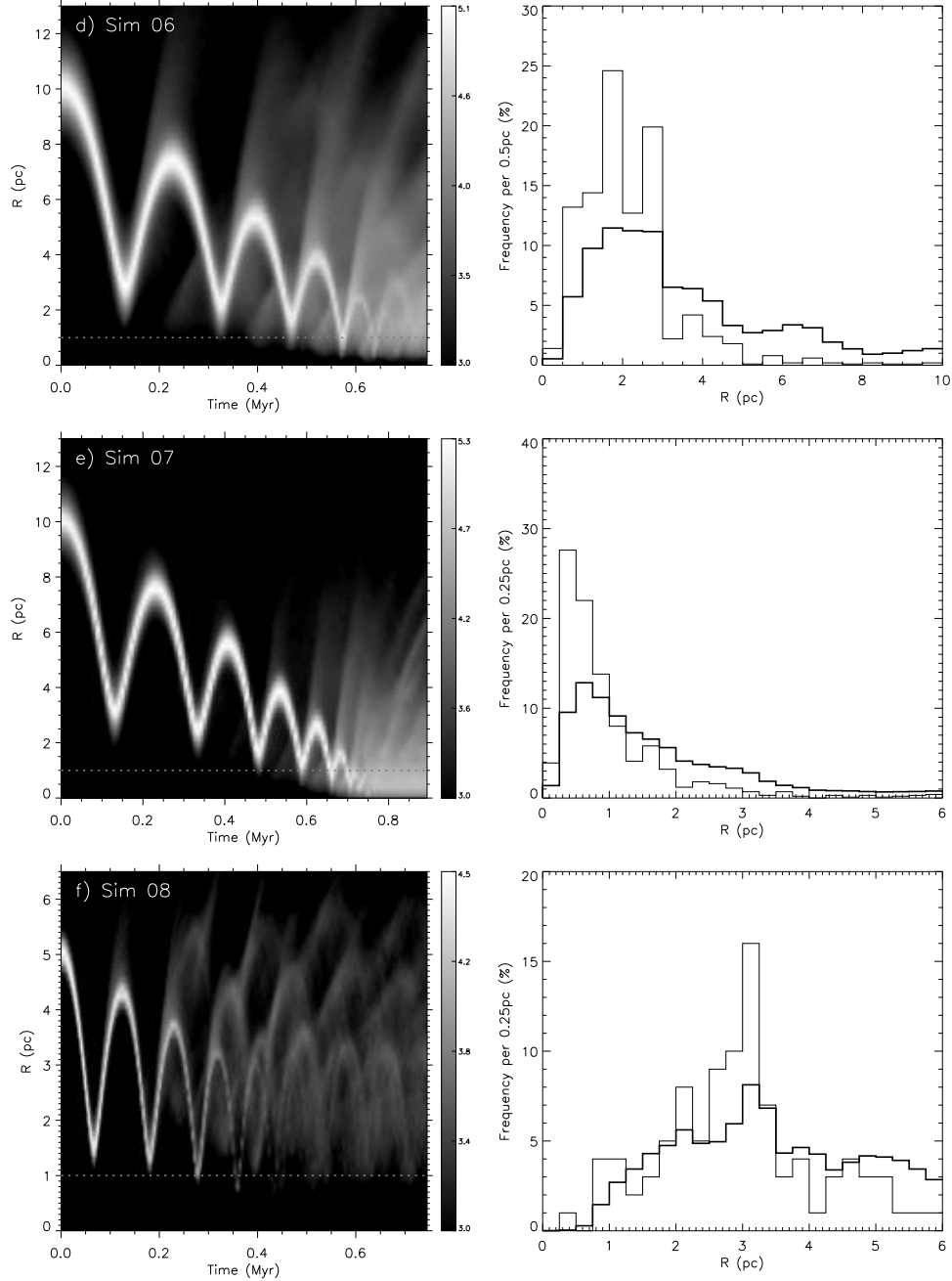
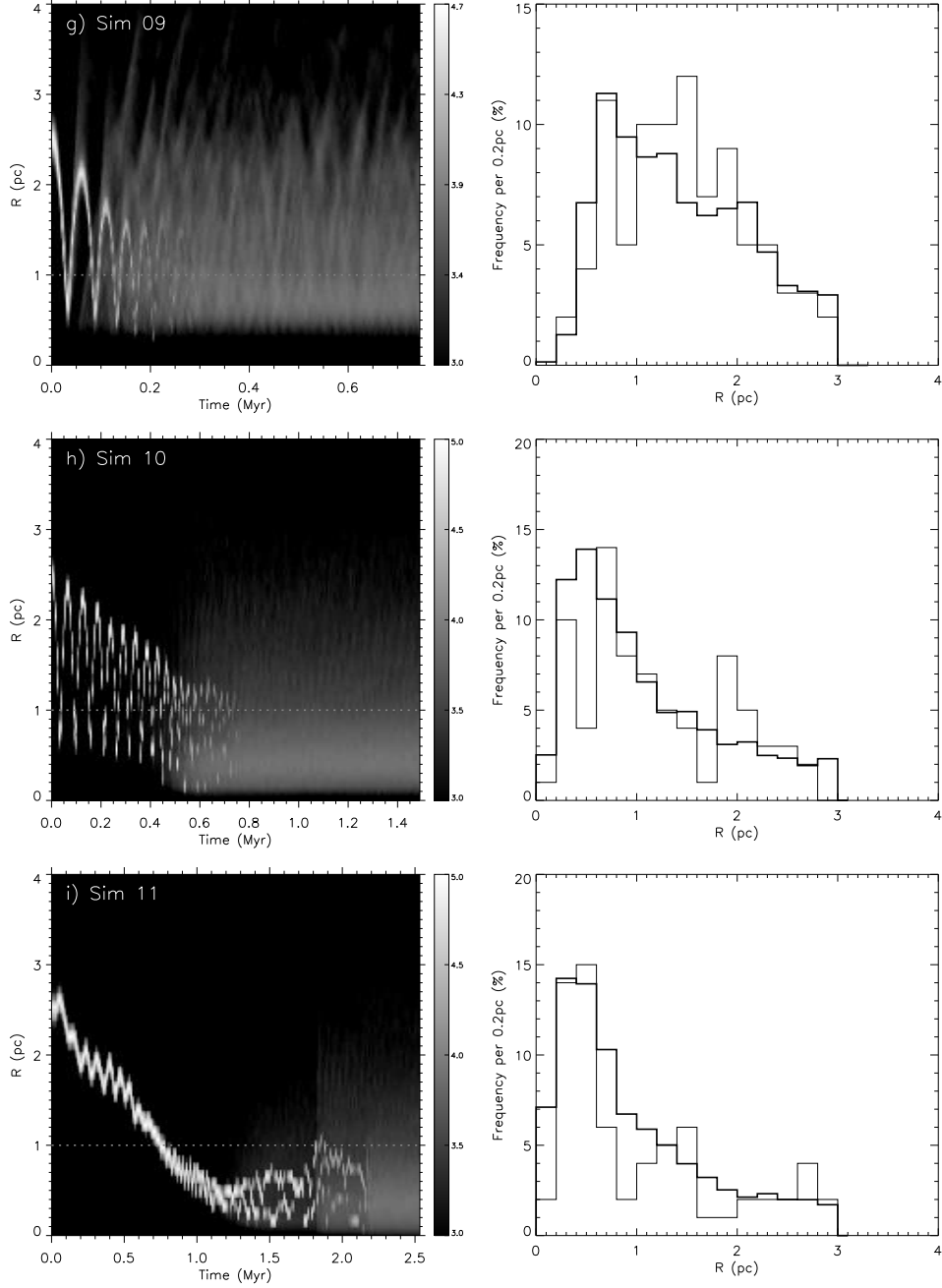


FIG. 2 (continued).—

Smaller clusters having a higher central concentration and initially located relatively near the GC (Simulations 10–13;  $M_{cl} = 10^5$ ,  $R = 2.5 - 10$  pc, &  $\rho_c = 1.3 \times 10^8 M_\odot pc^{-3}$ ) are found to be *potentially* another set of candidates for the central parsec cluster. Unlike the  $10^6 M_\odot$  clusters, however, the stars initially located in the innermost 1% of the cluster core of these “low-mass” clusters have a final concentration to the central parsec of the GC similar to that of the entire population of cluster stars,  $\sim 50\%$ . Also, one must keep in mind that even these “low-mass” clusters are an order of magnitude more massive than the massive Arches and Quintuplet clusters.

We have found that the  $10^5$  and  $10^6 M_\odot$  clusters have too many He I stars compared to the number found in the central parsec and the surrounding volume. A  $10^4 M_\odot$  cluster composed of only stars, on the other hand, would have the appropriate number of He I stars, but it would not experience significant dynamical friction before complete cluster evaporation, as the frictional deceleration is expected to scale as  $M_{cl}^{-1}$ . Thus it appears that, in order for dynamical friction to be responsible for the central parsec cluster, the total cluster mass should be  $\gtrsim 10^5 M_\odot$ , and some phenomenon must be invoked in order to reduce the number of He I stars. Perhaps most of them have disappeared as supernovae, while others have



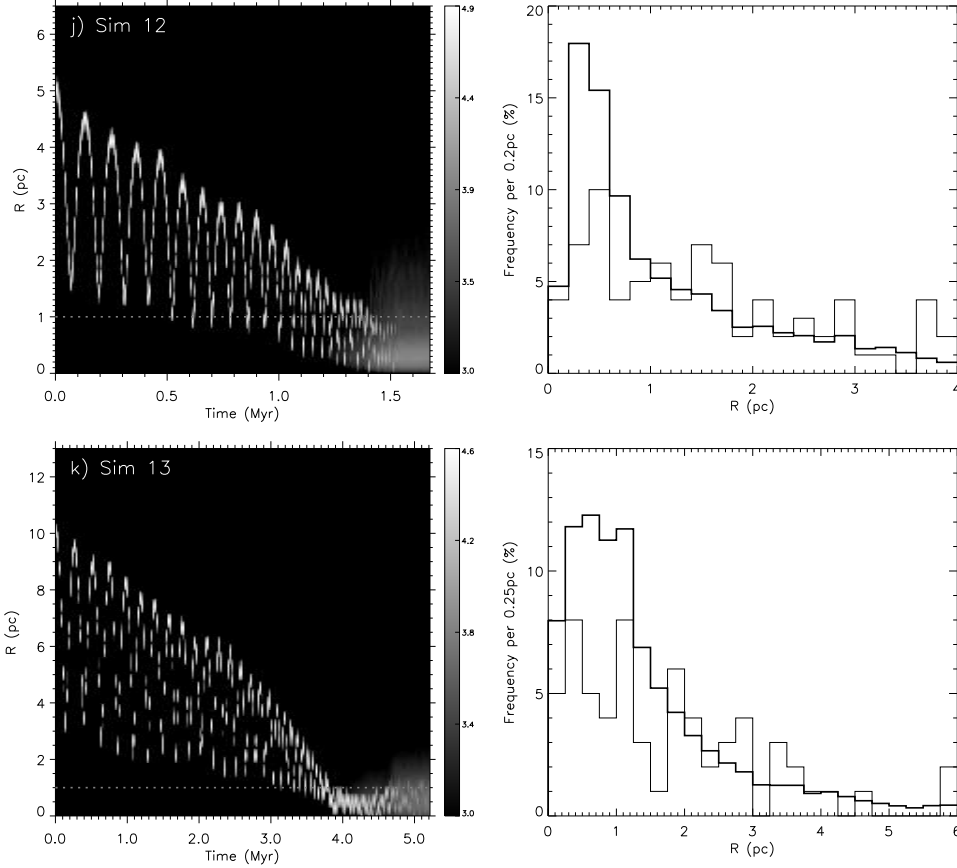
FIG. 2 (*continued*).—

been lost by evaporation at a rate which exceeds that in our models. The evaporation hypothesis, however, leaves us with the embarrassment that large numbers of massive He I stars should have been detected (Figer 1995). Another possible explanation is that the lower mass limit for He I stars is higher than is usually considered to be the case. Finally, the possibility has been raised that a significant number of massive stars have merged in the dense stellar core to form an intermediate-mass black hole (Portegies Zwart & McMillan 2002; Hansen & Milosavljevic 2003).

The large cluster mass required for the hypothesis that dynamical friction is responsible for bringing the central

young cluster into the central parsec is not a problem in principle. While there exists no known, young cluster near the center of our Galaxy having a mass within an order of magnitude of that required, such massive clusters have been found in many other – usually starburst – galaxies, and are usually referred to as super star clusters.

Finally, we note that, if the dynamical friction hypothesis is applicable to luminous young stars in the central parsec, then the collapsed core of the original cluster might still be present there. The finding of a very compact configuration of massive stars in the central parsec would strengthen this hypothesis considerably.

FIG. 2 (*continued*).—

In conclusion, we have identified a few simulations that can be regarded as candidates for the origin of the central parsec cluster. However, the required conditions are rather extreme. While it is more probable for a massive cluster ( $10^6 M_\odot$ ) to reach the central parsec before disruption, one needs a finely-tuned set of parameters to observe only  $\sim 16$  He I stars out of the whole original mass and to have them be concentrated almost entirely into the central parsec. Less massive clusters ( $10^5 M_\odot$ ) might have less problem with the He I star count, but require either an extremely high initial central density (inherently or via relaxation) or a rapid segregation of massive stars in the cluster core. Consideration of internal dynamics and mass spectrum in the cluster will enable core collapse and mass segregation and thus tend to raise the probability for the cluster core to reach the central parsec intact, but these same effects also make the cluster evaporate more quickly and thus weaken the drag from dynamical friction, thus lowering that probability. The internal dynamics of the cluster are more important for a more compact cluster located at a larger  $R$ . We have artificially and partially explored one of the consequences of the internal cluster dynamics by trying some

models with extremely high central densities. However, numerical simulations that can handle both the galactic scale (dynamical friction) and the cluster scale (internal cluster dynamics) are still needed to show the exact role of the internal dynamics for the structural evolution of our cluster models for the time intervals considered here.

S.S.K. thanks Michael Fellhauer, Hyung Mok Lee, David Merritt, Andres Meza, and Martin Weinberg for helpful discussion. M.M. acknowledges interesting and fruitful conversations with Oertwin Gerhard and Simon Portegies-Zwart. We are grateful to Gaber Mohamed at Academic Technology Services (ATS) of UCLA for his kind assistance with issues on supercomputing. We have used computer facilities at ATS of UCLA, San Diego Supercomputer Center, and Maui High Performance Computing Center of the University of New Mexico. Work by S.S.K. was supported by the Astrophysical Research Center for the Structure and Evolution of the Cosmos (ARCSEC) of Korea Science and Engineering Foundation through the Science Research Center (SRC) program.

## REFERENCES

- Athanassoula, E., Fady, E., Lambert, J. C., & Bosma, A. 2000, MNRAS, 314, 475
- Binney, J. & Tremaine, S. 1987, Galactic dynamics (Princeton: Princeton University Press)
- Bonnell, I. A., Bate, M. R., Clarke, C. J., & Pringle, J. E. 1997, MNRAS, 285, 201
- Chandrasekhar, S. 1943, ApJ, 97, 255

- Cotera, A. S., Erickson, E. F., Colgan, S. W. J., Simpson, J. P., & Allen, D. A. 1996, *ApJ*, 461, 750
- Cotera, A. S., Simpson, J. P., Erickson, E.F., Colgan, S. W. J., Burton, M. G. & Allen, D.A. 1999, *ApJ*, 510, 747
- Eckart, A., Ott, T., & Genzel, R. 1999, *A&A*, 352, L22
- Figer, D. F. 1995, Ph.D. thesis, UCLA
- Figer, D. F., Kim, S. S., Morris, M., Serabyn, E., Rich, R. M., & McLean, I. S. 1999, *ApJ*, 525, 750
- Figer, D. F., McLean, I. S., & Morris, M. 1995, *ApJ*, 447, L29
- Figer, D. F., McLean, I. S., & Morris, M. 1999, *ApJ*, 514, 202
- Fukushige, T., & Heggie, D. C. 2000, *MNRAS*, 318, 753
- Genzel, R., Thatte, N., Krabbe, A., Kroker, H., & Tacconi-Garman, L. E. 1996, *ApJ*, 472, 153
- Gerhard, O. 2001, *ApJ*, 546, L39
- Glass, I. S., Moneti, A., & Moorwood, A. F. M. 1990, *MNRAS*, 242, 55P
- Hansen, B. M. S., & Milosavljevic, M. 2003, submitted , /astro-ph/0306074/
- Jackson, J. M., et al. 1993, *ApJ* 402, 173
- Jenkins, A., & Binney, J. 1994, *MNRAS*, 270, 703
- Kim, S. S., Morris, M., & Lee, H. M. 1999, *ApJ*, 525, 228
- Kim, S. S., Figer, D. F., Lee, H. M., & Morris, M. 2000, *ApJ*, 545, 301
- King, I. 1966, *AJ*, 71, 276
- Krabbe, A. et al. 1995, *ApJ*, 447, L95
- Kroupa, P. 2001, *MNRAS*, 322, 231
- Lin, D. N. C., & Tremaine, S. 1983, *ApJ*, 264, 364
- Lindqvist, M., Habing, H. J., & Winnberg, A. 1992, *A&A*, 259, 118
- Lynden-Bell, D. 1960, *MNRAS*, 120, 204
- Merritt, D. 1996, *AJ*, 111, 2462
- Murray, S. D., & Lin, D. N. C. 1996, *ApJ*, 467, 728
- Morris, M. 1993, *ApJ*, 408, 496
- Morris, M., Ghez, A. M. & Becklin, E. E. 1999, *Adv. Spa. Res.* 23, 959
- Morris, M., & Serabyn, E. 1996, *ARA&A*, 34, 645
- Nagata, T., Woodward, C. E., Shure, M., Pipher, J. L., & Okuda, H. 1990, *ApJ*, 351, 83
- Nagata, T., Woodward, C. E., Shure, M., & Kobayashi, N. 1995, *AJ*, 109, 1676
- Okuda, H., et al. 1990, *ApJ*, 351, 89
- Paumard, T., Maillard, J. P., Morris, M. & Rigaut, F. 2001, *A&A*, 366, 466
- Portegies Zwart, S. F., & McMillan, S. L. 2002, *ApJ*, 576, 899
- Sanders, R. H. 1998, *MNRAS* 296, 1009
- Schaller, G., Schaerer, D., Meynet, G., & Maeder, A. 1992, *A&AS*, 96, 269
- Springel V., Yoshida N., & White S. D. M., 2001, *New Astronomy*, 6, 79
- Takahashi, K., & Portegies Zwart, S. F. 1998, *ApJ*, 503, L49
- White, S. D. M. 1976, *MNRAS*, 177, 717